



Discovery of novel hydroxy-thiazoles as HIF- α prolyl hydroxylase inhibitors: SAR, synthesis, and modeling evaluation

Christopher M. Tegley^{a,*}, Vellarkad N. Viswanadhan^a, Kaustav Biswas^a, Michael J. Frohn^a, Tanya A. N. Peterkin^a, Catherine Chang^a, Roland W. Bürli^a, Jennifer H. Dao^a, Henrike Veith^b, Norma Rogers^b, Sean C. Yoder^b, Gloria Biddlecome^b, Philip Tagari^a, Jennifer R. Allen^a, Randall W. Hungate^a

^a Chemistry Research and Discovery, Amgen, Inc., One Amgen Center Drive, Thousand Oaks, CA 91320, USA

^b Hematology, Amgen, Inc., One Amgen Center Drive, Thousand Oaks, CA 91320, USA

ARTICLE INFO

Article history:

Received 23 May 2008

Revised 10 June 2008

Accepted 10 June 2008

Available online 13 June 2008

Keywords:

Prolyl hydroxylase inhibitors

HIF-1 α

Hypoxia

Ischemia

Anemia

Peripheral arterial disease

Myocardial infarction

Stroke

Diabetes

Hydroxy-thiazole

ABSTRACT

Inhibition of the PHD2 enzyme has been associated with increased red blood cell levels. From a screening hit, a series of novel hydroxyl-thiazoles were developed as potent PHD2 inhibitors.

© 2008 Elsevier Ltd. All rights reserved.

Hypoxia-inducible factor (HIF) is a transcription factor and key regulator of cellular responses to hypoxia in a wide variety of organisms.¹ Among the genes regulated by HIF transcriptional activity, many play crucial roles in angiogenesis, erythropoiesis, energy utilization, vascular tone, apoptosis and cellular proliferation. HIF can also be involved in pathophysiological conditions like cancers, where it is commonly elevated due to genetic alterations or tumor hypoxia.²

The HIF transcription factor consists of an α/β heterodimer that binds to hypoxia-response elements within HIF target genes to control transcription.³ HIF- β is a constitutive nuclear protein that dimerizes with oxygen-regulated HIF- α subunits. HIF- α is a constitutively produced protein whose stability is primarily regulated by cellular pO_2 . At physiological pO_2 , HIF- α is hydroxylated on conserved proline residues (Pro402 and Pro564 on human HIF-1 α). This proline hydroxylation creates recognition sites for the von Hippel-Lindau protein which targets HIF- α for poly-ubiquitination and subsequent proteasomal degradation.⁴ Proline hydroxylation

is catalyzed by HIF prolyl hydroxylase domain enzymes (PHD1, 2, 3) in a reaction that requires Fe(II), 2-oxoglutarate (2-OG), and O_2 .⁵ As pO_2 falls, HIF- α is poorly hydroxylated, protein degradation is blunted, and HIF-mediated transcription occurs.

It is thought that stabilization of HIF- α by inhibition of PHD enzymes could be a viable therapy for anemia, for ischemic diseases including myocardial infarction, stroke, peripheral arterial disease, or for complications of diabetes.⁶ PHD2 is considered the key enzyme for HIF- α regulation in a variety of cell lines⁷ and for stimulating erythropoiesis.⁸ For these reasons, we initiated a medicinal chemistry program aimed at the identification and optimization of potent PHD2 inhibitors (see Fig. 1).

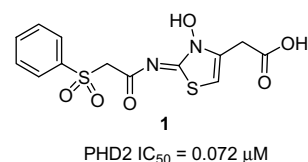


Figure 1. Screening hit hydroxy-thiazole 1.

* Corresponding author. Tel.: +1 805 447 0622; fax +1 805 480 3016.

E-mail address: ctegley@amgen.com (C.M. Tegley).

We undertook a high throughput screen (HTS) of our internal compound collection utilizing a homogeneous time-resolved fluorescence resonance energy transfer (TR-FRET) assay to test for PHD2 inhibition. This assay detects PHD2-dependent hydroxylation of Pro564 in a peptide derived from human HIF-1 α .⁹ We identified compound **1** as a possible starting point for SAR studies to optimize the potency of this novel class of PHD2 inhibitor.

Table 1 highlights modifications to the carboxylate side-chain and thiazole ring. The importance of both the hydroxy-thiazole moiety and the carboxylate for PHD2 inhibition are evident in compounds **2**, **3**, and **4** which lack activity. Mono-methylation of the carboxylate side-chain resulted in a >18-fold decrease in activity relative to compound **1** as shown by compound **11**, whereas the gem-dimethyl analog **12** resulted in a complete loss of inhibitory activity. In addition, methylation of the thiazole ring (compound **13**) and homolog **14** resulted in a >5-fold decrease in potency for both compounds when compared to the lead compound **1**.

With preliminary SAR established, our strategy was to maintain the hydroxy-thiazole carboxylate as our core scaffold and examine substitution effects on the amide side-chain and sulfonyl group substitution.

We attempted to replace the sulfonyl group with an alternate linker to the distal phenyl group. As shown in Table 2, replacement of the sulfone with a sulfide **15** resulted in a greater than 30-fold decrease in potency. Substitution of the sulfone with an ether **16** or amine **17** retained weak activity whereas the phenethyl analog **18** resulted in a complete loss of inhibitory activity.

The structure–activity relationships of phenyl group substitution are highlighted in Table 3. Replacement of the phenyl group

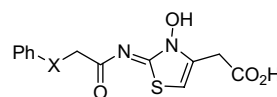
Table 1
Structure–activity relationship of hydroxy-thiazole carboxylate^a

Compound	Structure	PHD2 IC ₅₀ ^b (μM)
1		0.072 ± 0.026
2		>40
3		>40
4		>40
11		1.3 ± 0.58
12		>40
13		0.40 ± 0.23
14		0.41 ± 0.22

^a IC₅₀ values represent an average of at least three titrations ± SD.

^b Assay details to be published elsewhere (Ref. 9).

Table 2
Structure–activity relationship of amide side-chain^a



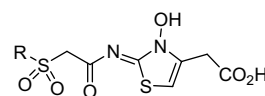
Compound	X	PHD2 IC ₅₀ ^b (μM)
1	SO ₂	0.072 ± 0.026
15	S	2.3 ± 1.6
16	O	4.4 ± 0.68 ^c
17	NH	1.7 ± 0.19 ^c
18	CH ₂	>40

^a IC₅₀ values represent an average of at least three titrations ± SD.

^b Assay details to be published elsewhere (Ref. 9).

^c Mean value from two experiments.

Table 3
Structure–activity relationship of sulfone substitution^a



Compound	R	PHD2 IC ₅₀ ^b (μM)
1	Ph	0.072 ± 0.026
19	Me	0.600 ± 0.089 ^c
20	4-Me-Ph	0.050 ± 0.023
21	4- ^t Bu-Ph	0.021 ± 0.009
22	2-Cl-Ph	0.072 ± 0.010
23	3-Cl-Ph	0.098 ± 0.013
24	4-Cl-Ph	0.033 ± 0.001
25	2-Naphthyl	0.027 ± 0.012
26	4-Ph-Ph	0.021 ± 0.008
27	Bn	0.011 ± 0.009
28	4- ^t Bu-Bn	0.003 ± 0.002

^a IC₅₀ values represent an average of at least three titrations ± SD.

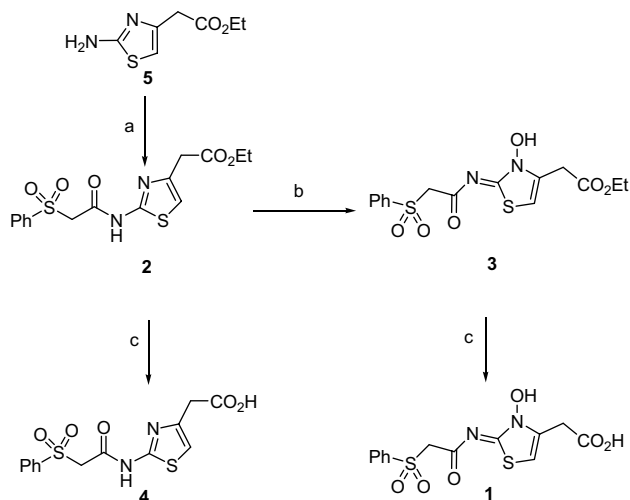
^b Assay details to be published elsewhere (Ref. 9).

^c Mean value from two experiments.

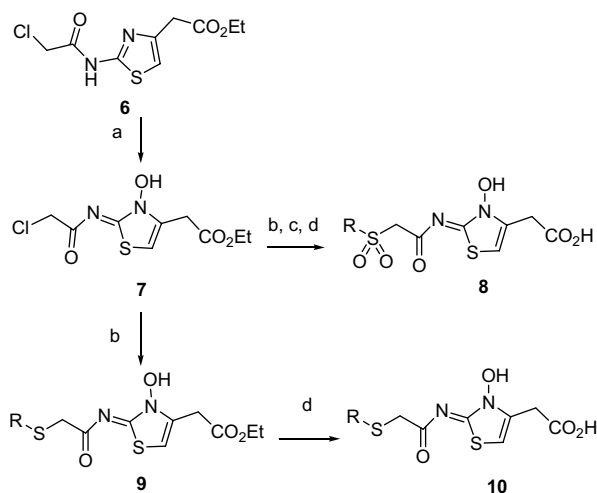
with a methyl group shown by compound **19** resulted in an 8-fold decrease in potency relative to compound **1**. Substitution around the distal phenyl group was varied to understand the role of electronic and hydrophobic substitution effects on inhibitory activity. Electron-donating groups such as the *para*-methyl analog **20** had a modest effect on activity whereas the *para*-chloro analog **24** was slightly more potent than compound **1** and may be slightly more potent than the *ortho*-chloro **22**, and *meta*-chloro **23** analogs. The potency of the 4-*tert*-butyl-phenyl analog **21** (IC₅₀ = 21 nM) led us to further extend the hydrophobic substituents. The 2-naphthyl analog **25** and 4-biphenyl analogs **26** showed at least a 2-fold improvement in potency relative to compound **1**. A significant increase in potency was seen with the benzyl sulfone analog **27** which showed a 7-fold improvement in potency compared to compound **1**. Further optimization of compound **27** was achieved as shown by compound **28** (IC₅₀ = 3 nM) which demonstrated a greater than 20-fold increase in potency compared to compound **1**.

Altogether the SAR studies showed that changes to the hydroxy-thiazole and to the side chain resulted in a decrease in potency whereas extension of the distal hydrophobic substituents resulted in a significant improvement in potency.

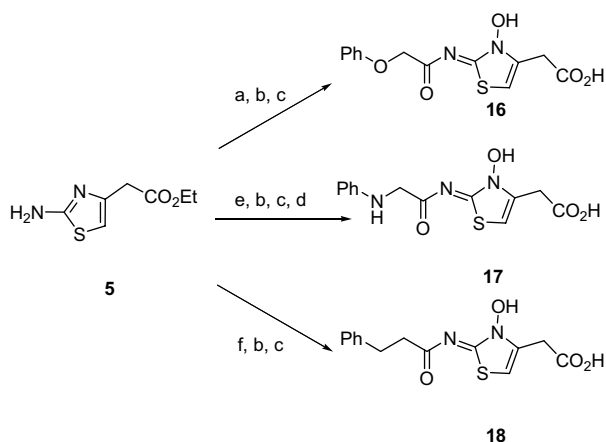
To enable SAR exploration of this novel class of PHD2 inhibitors, three synthetic routes (Schemes 1–3) were developed. Analogs were prepared according to Scheme 1 when the sulfonyl acetic acid intermediates were commercially available. Ethyl 2-aminothiazole-4-acetate **5** was coupled to phenyl sulfonyl acetic acid to afford the thiazole ethyl ester **2** which was subsequently oxidized



Scheme 1. Reagents and conditions: (a) $\text{PhSO}_2\text{CH}_2\text{CO}_2\text{H}$, EDC, Et_3N , DCM, rt, 80%; (b) Oxone[®], MeOH, H_2O , rt, 40%; (c) aq NaOH, THF, rt, 100%.



Scheme 2. Reagents and conditions: (a) MCPBA, CHCl_3 , rt, 90%; (b) R-SH, Et_3N , THF, 40–99%; (c) Oxone[®], EtOH, H_2O , rt; (d) aq NaOH, THF, rt, 100%.



Scheme 3. Reagents and conditions: (a) $\text{PhOCH}_2\text{CO}_2\text{H}$, HATU, DIPEA, DMF, rt, 94%; (b) Oxone[®], MeOH, H_2O , rt, 20–36%; (c) aq NaOH, THF, rt, 38–88%; (d) HCl, dioxane, rt, 88%; (e) $\text{PhN}(\text{Boc})\text{CH}_2\text{CO}_2\text{H}$, HATU, DIPEA, DMF, rt, 58%; (f) $\text{Ph}(\text{CH}_2)_2\text{CO}_2\text{H}$, TBUTU, DIPEA, DMF, rt, 100%.

with Oxone[®] to give the hydroxy-thiazole ester **3** and finally hydrolyzed to give the hydroxy-thiazole carboxylate **1**. Lastly, compound **2** was hydrolyzed to afford the thiazole carboxylate **4**.

When the sulfonyl acetic acid intermediates were not available, the synthetic route depicted in Scheme 2 was utilized to take advantage of commercially available substituted thio-phenols. MCPBA oxidation of ethyl 2-(2-chloroacetamido)-4-thiazoleacetate **6** afforded the intermediate hydroxy-thiazole **7**.¹⁰ Hydroxy-thiazole **7** was then reacted with substituted aryl thiols to give analogs **10** after hydrolysis. The sulfide-analogs could also be oxidized with Oxone[®] to give the sulfone-analogs **8** after hydrolysis.

Scheme 3 shows the synthetic schemes used to prepare each of the amide side-chain analogs **16**, **17**, and **18**. Ethyl 2-aminothiazole-4-acetate **5** was coupled with either phenoxyacetic acid, *N*-Boc-*N*-phenyl glycine or 3-phenyl-*n*-propionic acid then oxidized with Oxone[®] and hydrolyzed. The Boc-protected precursor to analog **17** was de-protected with HCl/dioxane in the final step.

To leverage our medicinal chemistry effort we decided to use our recently published X-ray crystal structure of the catalytic domain of human PHD2 co-crystallized with a 2-OG-competitive isoquinoline inhibitor.¹¹ The active site is lined by a number of hydrophobic residues. In addition, several polar residues and water molecules line the pocket and interact with the ligand and Fe(II) in the active site. Ample evidence,¹² suggests coordination of Fe(II) and a salt bridge involving Arg383 as key elements for potent PHD2 inhibition.

As a first step to assess the binding modes of hydroxy-thiazoles **1**, a conformational analysis was performed and showed two minima equal in energy with the barrier to rotation (in the absence of Fe) about the N-carbonyl bond of 18 kcal/mol. Potential binding modes corresponding to these minima were considered, based on overlays with the X-ray structure of the isoquinoline compound. Although, there is no difference in energy between the two conformers (Fig. 2), the geometry of the hydroxyl thiazolyldene acetamide represented in binding mode 1, corresponded to the single crystal X-ray structure of compound **1** (Fig. 3).¹³

Figures 4 and 5 show the putative binding modes corresponding to the two different conformations of the core group, following optimization of the two complexes.¹⁴ Both binding modes confirmed the salt bridge between the carboxylate group and Arg383, penetrating a tight pocket lined by several hydrophobic residues. The binding mode 1 (Fig. 4) showed the aryl group attached to the sulfone making hydrophobic contacts with Ile256, Trp258, Met299 and Tyr310. The binding mode 2 (Fig. 5) also revealed contacts with Tyr310 and other hydrophobic residues. An important distinction between the two putative binding modes,

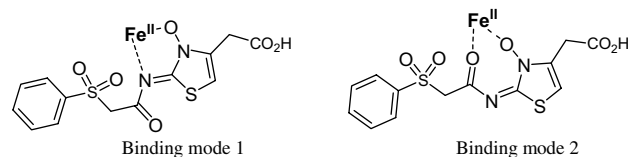


Figure 2. Two possible binding modes of compound **1**.

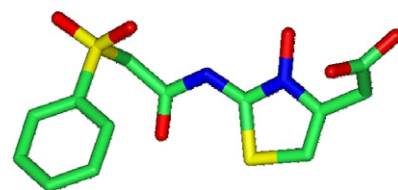


Figure 3. Single crystal X-ray structure of **1**.

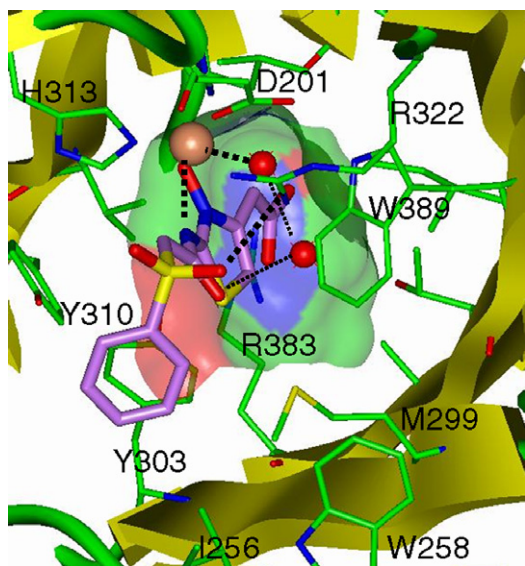


Figure 4. Binding mode 1 of the lead compound **1**, shown in pink. The inner pocket containing the acid group of the ligand, making a salt bridge with Arg383. The inner pocket is shown as a Connolly semi-transparent surface for the residues lining the pocket, color coded in atom colors of the closest atom type. Fe(II) ion is identified as an orange sphere and crystallographic waters within the active site are identified as red spheres. Some important protein residues are identified. The protein main chain is shown, rendered by its secondary structure.

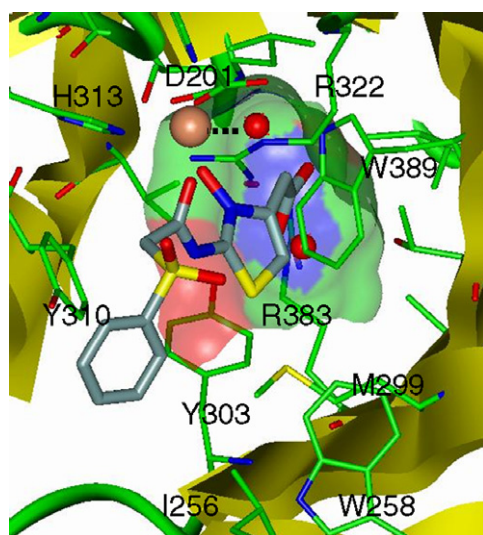


Figure 5. Binding mode 2 of the lead compound **1**, shown in gray.

is a potential interaction of Arg389 with the sulfone in binding mode 1 that is absent in binding mode 2. Due to these reasons, we speculated that the binding mode with the exocyclic nitrogen facing Fe (II) was more probable.

Our modeling and SAR studies are in agreement that the hydroxy-thiazole and carboxylate moieties are key binding elements that mimic 2-OG in the binding site and are important elements for PHD2 inhibition. Changes to the lead compound **1** that disrupt either the coordination with Fe(II) or the salt bridge with Arg383 leads to a significant decrease in potency. The importance of the sulfone moiety hypothesized in the binding model may be noted and is in agreement with the observed SAR. The significant improvement in potency achieved, via extension of the distal

hydrophobic substituents, can be attributed to favorable interactions with lipophilic residues that line the active site.

In summary, we discovered a novel PHD2 inhibitor **1** ($IC_{50} = 72$ nM) via high throughput screening. Through SAR studies, we successfully optimized the potency of the lead compound **1** by over 20-fold as shown by compound **28** ($IC_{50} = 3$ nM). In addition, modeling studies provided insight into the possible binding mode of this novel class of PHD2 inhibitors. Description of in vivo properties of analogs in this series will be the subject of future publications.

Acknowledgement

We thank Dr. Richard J. Staples for the single crystal X-ray of compound **1**.

Supplementary data

Supplementary data associated with this article can be found, in the online version, at doi:10.1016/j.bmcl.2008.06.031.

References and notes

- (a) Bruick, R. K. *Genes Dev.* **2003**, *17*, 2614; (b) Safran, M.; Kaelin, W. G. *J. Clin. Invest.* **2003**, *111*, 779; (c) Semenza, G. L. *Physiology* **2004**, *19*, 176; (d) Schofield, C. J.; Ratcliffe, P. J. *Nat. Rev. Mol. Cell Biol.* **2004**, *5*, 343.
- (a) Pugh, C. W.; Ratcliffe, P. J. *Nat. Med.* **2003**, *9*, 677; (b) Semenza, G. L. *Nat. Rev. Cancer* **2003**, *3*, 721.
- Wenger, R. H.; Stiehl, D. P.; Camenisch, G. *Science's STKE* **2005**, 306, re12.
- (a) Jaakkola, P.; Mole, D. R.; Tian, Y. M.; Wilson, M. I.; Gielbert, J.; Gaskell, S. J.; von Kriegsheim, A.; Hebestreit, H. F.; Mukherji, M.; Schofield, C. J.; Maxwell, P. H.; Pugh, C. W.; Ratcliffe, P. J. *Science* **2001**, *292*, 468; (b) Ivan, M.; Kondo, K.; Yang, H. F.; Kim, W.; Valiando, J.; Ohh, M.; Salic, A.; Asara, J. M.; Lane, W. S.; Kaelin, W. G. *Science* **2001**, *292*, 464; (c) Semenza, G. L. *Nat. Rev. Cancer* **2003**, *3*, 721.
- Epstein, A. C. R.; Gleadle, J. M.; McNeill, L. A.; Hewitson, K. S.; O'Rourke, J.; Mole, D. R.; Mukherji, M.; Metzzen, E.; Wilson, M. I.; Dhanda, A.; Tian, Y.-M.; Masson, N.; Hamilton, D. L.; Jaakkola, P.; Bartstead, R.; Hodgkin, J.; Maxwell, P. H.; Pugh, C. W.; Schofield, C. J.; Ratcliffe, P. J. *Cell* **2001**, *107*, 43.
- Hewitson, K. S.; McNeill, L. A.; Schofield, C. J. *Curr. Pharm. Des.* **2004**, *10*, 821.
- Appelhoff, R. J.; Tian, Y.-M.; Raval, R. R.; Turley, H.; Harris, A. L.; Pugh, C. W.; Ratcliffe, P. J.; Gleadle, J. M. *J. Biol. Chem.* **2004**, *279*, 38458.
- (a) Percy, M. J.; Zhao, Q.; Flores, A.; Harrison, C.; Lappin, T. R. J.; Maxwell, P. H.; McMullin, M. F.; Lee, F. S. *Proc. Natl. Acad. Sci. U.S.A.* **2006**, *103*, 654; (b) Percy, M. J.; Furlow, P. W.; Beer, P. A.; Lappin, T. R. J.; McMullin, M. F.; Lee, F. S. *Blood* **2007**, *110*, 2193; (c) Minamishima, Y. A.; Moslehi, J.; Bardeesy, N.; Cullen, D.; Bronson, R. T.; Kaelin, W. G., Jr. *Blood* **2008**, *111*, 3236.
- Dao, J. H.; Kurzeja, R. J. M.; Morachis, J. M.; Veith, H.; Lewis, J.; Yu, V.; Tegley, C.; Tagari, P. *Anal. Biochem.*, submitted for publication.
- Perrone, E.; Alpegiani, M.; Giudici, F.; Bedeschi, A.; Pellizzato, R.; Nannini, G. *J. Heterocycl. Chem.* **1984**, *21*, 1097.
- McDonough, M. A.; Li, V.; Flashman, E.; Chowdhury, R.; Mohr, C.; Lienard, B. M. R.; Zondlo, J.; Oldham, N. J.; Clifton, I. J.; Lewis, J.; McNeill, L. A.; Kurzeja, R. J. M.; Hewitson, K. S.; Yang, E.; Jordon, S.; Syed, R. S.; Schofield, C. J. *Proc. Natl. Acad. Sci. U.S.A.* **2006**, *103*, 9814.
- (a) Mole, D. R.; Schlemminger, I.; McNeill, L. A.; Hewitson, K. S.; Pugh, C. W.; Ratcliffe, P. J. *Bioorg. Med. Chem. Lett.* **2003**, *13*, 2677; (b) Warshakoon, N. C.; Wu, S.; Boyer, A.; Kawamoto, R.; Sheville, J.; Renock, S.; Xu, K.; Pokross, M.; Zhou, S.; Winter, C.; Walter, R.; Mekel, M.; Evdokimov, A. G. *Bioorg. Med. Chem. Lett.* **2006**, *16*, 5517; (c) Warshakoon, N. C.; Wu, S.; Boyer, A.; Kawamoto, R.; Sheville, J.; Renock, S.; Xu, K.; Pokross, M.; Evdokimov, A. G.; Walter, R.; Mekel, M.; *Bioorg. Med. Chem. Lett.* **2006**, *16*, 5598; (d) Warshakoon, N. C.; Wu, S.; Boyer, A.; Kawamoto, R.; Sheville, J.; Bhatt, R. T.; Renock, S.; Xu, K.; Pokross, M.; Zhou, S.; Walter, R.; Mekel, M.; Evdokimov, A. G.; East, S. *Bioorg. Med. Chem. Lett.* **2006**, *16*, 5616; (e) Warshakoon, N. C.; Wu, S.; Boyer, A.; Kawamoto, R.; Renock, S.; Xu, K.; Pokross, M.; Evdokimov, A. G.; Zhou, S.; Winter, C.; Walter, R.; Mekel, M. *Bioorg. Med. Chem. Lett.* **2006**, *16*, 5687.
- Crystallographic data has been deposited in the Cambridge Crystallographic Data Centre for small molecules and allocated the deposition number CCDC688161. Copies of data can be obtained free of charge on application to CCDC, 12 Union Road, Cambridge CB2 1EZ, UK.
- Modeling notes and references are contained in the supplementary material.